# Few-Cycle Soliton Pulse Compression in Lithium Niobate Nanophotonics

**Robert M. Gray,[1] Ryoto Sekine,[1] Maximilian Shen,[1] Thomas Zacharias,[1] James Williams,[1] Selina Zhou,[1] Rahul Chawlani,[1] Luis Ledezma,[1] Nicolas Englebert,[1] and Alireza Marandi[1,*]**

[1] *Department of Electrical Engineering, California Institute of Technology, Pasadena, CA 91125, USA*

[*] *marandi@caltech.edu*

**Abstract:** We experimentally demonstrate quadratic soliton compression in lithium niobate nanophotonic waveguides and achieve few-cycle pulses as short as ∼10 fs centered at 1 μm and 2 μm using sub-10 pJ of pump pulse energy. 

Ultrashort pulses with temporal widths on the order of femtoseconds, a few or even a single cycle of the carrier frequency [1], have enabled many research areas of interest including the measurement and control of electrons in materials [2, 3] , real-time characterization of ultrafast dynamics [4, 5], extreme nonlinear optics [6], and ultrafast information processing [7, 8]. Synthesis and control of ultrashort pulses typically involves, first, the generation of an ultra-broadband coherent spectrum followed by the spectral division, relative phase manipulation, and recombination of the segmented spectral components to generate ultrashort pulses [9]. These systems are usually implemented in bulk optics, are relatively complex, and require high pulse energies in the μJ regime which limits their scalability for real-life application.

One method towards reducing the number of system components is to utilize soliton pulse compression, in which nonlinear phase accumulation in spectral broadening is compensated by linear dispersive effects [10, 11]. Soliton pulse compression has typically been studied in media that have cubic (Kerr) nonlinearity, however this requires a suitable nonlinear medium with anomalous dispersion at the wavelength of interest. Alternatively, soliton pulse compression can be realized in quadratic nonlinear media, where phase-mismatched second harmonic generation (SHG) can enable compression down to the few-cycle regime [12], benefiting from the relatively stronger quadratic nonlinearity and flexibility in the dispersion sign. However, these systems are usually implemented in bulk optics in the cascading limit, where the required large phase-mismatch reduces the generated second-harmonic, and are limited by the presence of group-velocity mismatch (GVM) between the fundamental and second harmonic waves [13]. These limitations may be overcome in thin-film lithium niobate (TFLN) nanophotonics, where high-gain, dispersion-engineered waveguides have already facilitated the generation of multi-octave supercontinuum requiring low pump pulse energies in the pJ regime [14].

Here, we leverage these advantages of TFLN nanophotonics to overcome the challenges presented in bulk quadratic media and demonstrate two-color quadratic soliton pulse compression to the few-cycle regime. We design our device to achieve compression to near-single cycle widths at pulse energies on the order of a few pJ. By operating away from the cascading limit of large phase-mismatch, significant conversion to the second-harmonic soliton is observed. Our results pave the way towards the development of next-generation, scalable pulse synthesizers in integrated photonics.

The chip consists of x-cut, 700-nm MgO doped TFLN on a $SiO_2$ buffer layer. The resulting waveguide has a width of 2904 nm and etch depth of 330 nm resulting in a fundamental and second harmonic GVD of $\beta_\omega^{(2)}$ = 9.2 fs$^2$ /mm and $\beta_{2\omega}^{(2)}$ = 141 fs$^2$/mm, respectively, as well as a GVM of 27 fs/mm between the two waves. Additionally the fabricated waveguide consists of a 6.5-mm long periodically poled region with a poling period of 5.73 nm, with a phase-mismatch of $\Delta k = -4$ rad/mm.

The compression scheme is demonstrated in Fig. 1a, in which 35-fs pulses at the fundamental wavelength, 2090 nm, are coupled into the periodically poled waveguide and compressed via phase-mismatched interaction with the second harmonic. Experimental characterization of the pulses is done with a frequency-resolved-optical-gating (FROG) scheme based on non-collinear SHG and sum-frequency generation (SFG) in a 50 $\mu$m BBO crystal. A microscope image of the illuminated chip is shown in Fig. 1b.

We construct simulations of the coupled-wave equations using the Fourier split-step method which, given an input of a sech-shaped 35-fs pulse centered at 2090 nm (Fig. 1d), predicts the pulse evolution (Fig. 1c) as well as the the output second harmonic (Fig. 2e), fundamental (Fig. 1f), and combined (Fig. 1g) waves. The predicted pulse width of the fundamental and second harmonic are 7 fs, a single cycle of the carrier at 2090 nm, in good agreement with analytic predictions based on the variational soliton solutions given by Sukhorukov [15]. The width of the predicted combined output is 4 fs.

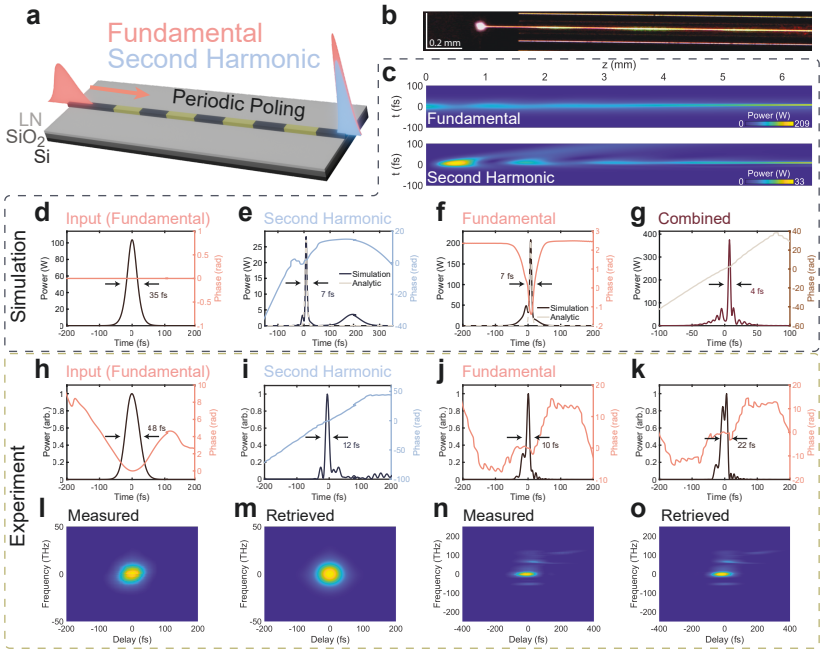


Fig. 1: **a)** A pulse at the fundamental frequency pumps the two-color soliton formation in the phase-mismatched nanophotonic waveguide. **b)** Microscope image of waveguide input, showing back-and-forth conversion. **c)** Simulated evolution of the fundamental (top) and second harmonic (bottom) as a function of propagation distance, z, in the waveguide. **d-f)** Simulation showing compression of the 35-fs fundamental input (**d**) to co-propagating 7-fs pulses at the second-harmonic (**e**) and fundamental (**f**). **g)** The resulting 4-fs combination of the fundamental and second harmonic. **h-k)** Experimental reconstructed temporal profiles. The 48-fs input at the fundamental (**h**) compresses to a 12-fs second-harmonic (**i**) and estimated 10-fs fundamental pulse (**j**), though phase ambiguities in the FROG can also result in a 22-fs reconstruction (**k**). **l-m)** Measured (**l**) and retrieved (**m**) SHG FROG traces of the fundamental input pulse. **n-o)** Measured (**n**) and retrieved (**o**) X-FROG traces of the compressor output.

The results of our compression measurement are shown in Figs. 1h-o. The input pulse, measured by using the SHG auto-FROG, is shown in Fig. 1h. It is a transform-limited 35-fs pulse around 2090 nm, which exhibits a slightly longer temporal width due to anomalous chirp from the optics leading up to the nonlinear crystal. The corresponding SHG FROG spectrogram is shown in Fig. 1l and qualitatively displays good agreement with the retrieval in Fig. 1m, exhibiting a reasonable FROG error of 0.0032.

The SFG X-FROG configuration is used to measure the output pulses, gated by a 100-fs pulse at 1045 nm from a commercial mode-locked laser. Shown in Fig. 1i, the retrieved second harmonic output pulse for a 5-pJ pump pulse is qualitatively similar to the simulation and exhibits a full-width at half-maximum (FWHM) of 12 fs. Due to phase ambiguities in the X-FROG, however, the recovered fundamental pulse is not consistent between runs of the PCGPA FROG retrieval algorithm. Most consistently, we observe something similar to the 10-fs pulse shown in Fig. 1j, but emergence of a second lobe which increases the FWHM to 22 fs is sometimes observed, as shown Fig. 1k. The 10-fs recovered pulse closely resembles the simulated results, while the 22-fs pulse does not, so we believe it is a more accurate representation of the compressed output. We believe the phase ambiguity is a consequence of the non-zero and unlocked $f_{ceo}$ of the pump laser, which causes a coherent beating between the spectrally overlapping fundamental and second-harmonic pulses over the course of the X-FROG measurement, resulting in a non-repeating input. Despite this ambiguity, the measured and retrieved X-FROG traces for the device output, shown in Figs. 1n-1o exhibit good qualitative agreement along with a reasonable FROG error of 0.0045. In conclusion, we have experimentally demonstrated two-color soliton pulse compression to less than two optical cycles of the carrier of the fundamental wave.

## References


1. Wirth *et al.*, Science **334**, 195–200 (2011).
2. Krausz *et al.*, Rev. modern physics **81**, 163–234 (2009).
3. Hui *et al.*, Nat. Photonics **16**, 33–37 (2022).
4. Pupeza *et al.*, Nature **577**, 52–59 (2020).
5. C. Riek *et al.*, Nature **541**, 376–379 (2017).
6. M. Wegener, *Extreme Nonlinear Optics: An Introduction*, Advanced Texts in Physics (Springer Berlin Heidelberg, 2006).
7. Leefmans *et al.*, Nat. Phys. **18**, 442–449 (2022).
8. Gray *et al.*, arXiv preprint arXiv:2405.17355 (2024).
9. Manzoni *et al.*, Laser & Photonics Rev. **9**, 129–171 (2015).
10. Colman *et al.*, Nat. Photonics **4**, 862–868 (2010).
11. Dudley *et al.*, Rev. modern physics **78**, 1135–1184 (2006).
12. Zhou *et al.*, Phys. review letters **109**, 043902 (2012).
13. Bache *et al.*, Opt. Express **16**, 3273–3287 (2008).
14. Jankowski *et al.*, APL Photonics **8** (2023).
15. A. A. Sukhorukov, Phys. Rev. E **61**, 4530 (2000).